Identification with a recombinant antibody of an inner-ear cytokeratin, a marker for hair-cell differentiation

Janet L. Cyr*†, Andrea M. Bell†, and A. J. Hudspeth†‡

†Howard Hughes Medical Institute and Laboratory of Sensory Neuroscience, The Rockefeller University, 1230 York Avenue, New York, NY 10021-6399

Extensive biochemical characterization of cells in the inner ear has been hampered by a lack of tools with which to identify inner-ear proteins. By using a single-chain antibody fragment isolated from a bacteriophage-displayed library, we have identified a cytokeratin that is abundant in nonsensory cells of the frog inner ear. Although the progenitors of hair cells exhibit strong immunoreactivity to this cytokeratin, the signal declines in immature hair cells and vanishes as the cells mature. The correlation between diminished immuno-reactivity and hair-cell differentiation indicates that the cytokeratin is down-regulated during the transition from a nonsensory to a sensory cell and suggests that the marker is an early index of hair-cell differentiation.

Our awareness of faint sounds and weak accelerations rests on the sensitivity of hair cells, which respond to subnanometer deflections of their hair bundles (1). The exquisite sensitivity of hair cells unfortunately renders them acutely susceptible to trauma from acoustical overstimulation. In addition, aminoglycoside antibiotics and some chemotherapeutic agents can damage or kill these sensory cells. Because they are postmitotic, hair cells can be replaced only by the differentiation of precursors. Although hair cells do not regenerate in the adult mammalian cochlea, replacement does occur in mammalian vestibular organs and more extensively in nonmammalian receptor organs (2, 3).

Little is known about the proteins involved in hair-cell differentiation and function. Although the identification and characterization of inner-ear proteins are impeded by the paucity of cells, the isolation of specific reagents directed against inner-ear proteins makes biochemical studies feasible. To generate such reagents, we produced a bacteriophage-displayed antibody-fragment library directed against proteins of the bullfrog inner ear (4). From this library, we isolated a single-chain Fv fragment (scFv) that specifically labels a protein expressed almost exclusively in the inner ear. We describe here the further characterization and identification of this protein as a cytokeratin whose expression declines during hair-cell differentiation.

Materials and Methods

The production of a library of bacteriophage-displayed scFvs and the selection of a clone producing an scFv with a high specificity for an inner-ear antigen have been described (4). For the present study, soluble scFvs from clone scFv-278 were isolated by the procedures in that reference.

Immunocytochemistry on Saccular Whole Mounts. Bullfrog sacculi were isolated and the otolithic membranes were mechanically removed. Sacculi were fixed for 1 h at 4°C in 4% (wt/vol) formaldehyde in PBS (68 mM NaCl/58 mM Na$_2$HPO$_4$/17 mM NaH$_2$PO$_4$, pH 7.4), rinsed in PBS, permeabilized for 1 h in PBS containing 1% (vol/vol) Triton X-100, and washed in PBS. Samples were blocked for 2 h in PBS containing 2.5% (vol/vol) Liquid Block (Amersham Pharmacia) and 3% (vol/vol) goat serum, then incubated overnight at 4°C in a mixture of 1.8 mg/liter affinity-purified scFv-278 and 1.5 mg/liter anti-epitope

tag antibody (E-tag antibody, Amersham Pharmacia) that was prepared at least 15 min in advance. After three 10-min washes with PBS containing 0.1% (vol/vol) Tween-20 (PBS-T), the samples were incubated for 2 h in PBS containing 2.5% (vol/vol) Liquid Block and 5 mg/liter of BODIPY-FL goat anti-mouse IgG (Molecular Probes) and washed three times with PBS-T. Sacculi were then incubated for 10 min in 125 μg/liter tetra-methylrhodamine B isothiocyanate-labeled phalloidin in PBS and washed in PBS. Images were obtained with an MRC-1000 confocal microscope (Bio-Rad) and were processed with NIH IMAGE (version 1.61; National Institutes of Health, Bethesda).

Immunocytochemistry with Isolated Hair Cells. Bullfrog saccular hair cells were enzymatically isolated (4) and allowed to settle onto cover slips previously exposed to 1 g/liter Con A. Cells were fixed for 20 min in 1% (wt/vol) formaldehyde in PBS, rinsed, and permeabilized for 20 min with 100 mg/liter saponin in PBS. Cells were processed for immunocytochemistry and imaged as indicated for saccular cryosections (4).

Expression Screening in Mammalian Cells. A bullfrog-saccular cDNA ZAP Express library, which contained 1.25×10^6 independent clones, was amplified and *in vivo* excised with ExAssist helper bacteriophage (Stratagene). The released bacteriophage were used to infect *Escherichia coli* strain XL1Blue (Stratagene) to generate subpools containing 10,000–60,000 clones each, which were amplified (5). Phagemid DNA from each subpool was used for transient transfection (LipofectAMINE, Life Technologies, Gaithersburg, MD) of tsA201 cells (6). At least 20 h later, the cells were fixed, permeabilized, and processed as described for isolated hair cells with 1.8 mg/liter affinity-purified scFv-278 and 1.5 mg/liter anti-epitope tag antibody. Bound scFv was detected with an anti-mouse antibody conjugated to alkaline phosphatase (1:200 dilution, Jackson ImmunoResearch) followed by reaction with BCIP/NBT (NEN). Positive cells were identified by light microscopy. XL1Blue MRF′ cells (Stratagene) were transformed with DNA from a positive subpool and were divided into smaller subpools; phagemid DNA was isolated and rescreened.

The 5′ end of the cDNA was isolated by using the PCR. Ten rounds of asymmetric PCR were performed with 48,000 plaque-forming units of the ZAP Express saccular cDNA library and 50 pmol of the sequence-specific Cytorev3 primer (5′-GGGT-

---

CAATCTCCAGATTAAGGG-3′) in a volume of 20 μl. Incubations at 94°C for 4 min, 60°C for 2 min, and 72°C for 2 min were followed by nine cycles at 94°C for 1 min, 60°C for 1 min, and 72°C for 1 min. Following amplification, additional components were added, including 50 pmol of vector primer (5′-TCACACAGGAAACAGCTATGACCTTGATTAGGCC-3′) and 20 pmol of Cytorev3 primer, to yield a final volume of 40 μl. This mixture was subjected to 30 cycles of amplification. Products were subcloned and sequenced. The 5′ end lacked an in-frame stop codon but included the presumptive translation-initiating Met based on sequence alignments with other cytokeratins. Sequence alignments were performed with MEGALIGN software (DNAstar, Madison, WI).

Immunoblots of Homogenates from Bullfrog and *Xenopus* Organs. Organs of the bullfrog and *Xenopus* were dissected, frozen in liquid nitrogen, and processed as described (4). Each lane of the SDS/PAGE gel contained 10 μg of protein. Parallel gels were stained to verify sample integrity.

Epitope Mapping. Deletion constructs of the cytokeratin cDNA were used to transfect tsA201 cells, which were then processed for immunocytochemistry as indicated for expression screening. One construct, Δ481–529, was generated by digestion of the original clone, which began at the codon for residue 66, with *Hin*dIII and *Kpn*I; this procedure resulted in a protein truncated after aa 480 but extended by nine irrelevant residues. An amino-terminal deletion construct, EGFP:168–393:FLAG, stemmed from digestion of the original clone with *Xma*I and *Kpn*I, which truncated the protein after residue 393. An epitope tag (FLAG epitope) was added to the carboxyl terminus of the cytokeratin sequence by annealing two oligonucleotides (5′-TCCCCCCGGGGAGTGTGATTATAAAGACGATGACG-ATAAAGGTACCCCG-3′ and 5′-CGGGGTACCTTTAT-CGTCATCGTCTTTATAATCACACTCCCGGGGGGGA-3′), digesting them with *Xma*I and *Kpn*I, and ligating them into the digested cytokeratin construct. To remove concatamers, we digested the product with *Kpn*I and religated it. After this product had been digested with *Pst*I and *Kpn*I, the fragment encoding the coiled-coil portion of the cytokeratin was ligated into the pEGFP-C3 vector (CLONTECH). This construct produced a protein consisting of enhanced green fluorescent protein (EGFP) followed by 10 irrelevant residues, cytokeratin residues 168–393, the FLAG epitope, and 11 irrelevant residues.

Electron-Microscopic Immunocytochemistry. Sacculi were dissected, fixed, permeabilized, treated with primary and secondary immune reagents, and washed as described for whole-mounted specimens. For the detection of bound scFv, specimens were exposed for 2 h to goat anti-mouse IgG conjugated to 10-nm gold beads (AuroProbe EM G10, Amersham Pharmacia) diluted 1:25 (vol/vol) in a solution of 2.5% (vol/vol) Liquid Block. After three washes in PBS-T and a 24-h wash in PBS at 4°C, the specimens were refixed for 2 h at 4°C with 100 mM glutaraldehyde in 100 mM sodium cacodylate (pH 7.4). After a wash, the tissue was postfixed for 1 h at 4°C with 50 mM OsO_4/10 mM $K_4Fe(CN)_6$ in the same buffer solution. The tissue was dehydrated in a graded series of ethanol concentrations and was stained *en bloc* with 0.5% (wt/vol) uranyl acetate in 70% ethanol. After further dehydration and passage through propylene oxide, specimens were embedded in epoxy plastic (EMbed 812, Electron Microscopy Sciences, Fort Washington, PA). Sections (60 nm) were stained with lead citrate and examined at 100 keV in an electron microscope (JEOL).

Results

Distribution of Immunoreactivity in the Sacculus and Other Inner-Ear Organs. In the bullfrog sacculus, a receptor organ for ground-borne vibration and low-frequency sound (7, 8), ≈2,500 hair cells

occur in a sensory epithelium, or macula, ≈1 mm in diameter. Although the mosaic of sensory and nonsensory cells is somewhat irregular, a mature hair cell is ordinarily encircled by six supporting cells in a roughly hexagonal lattice. New hair cells are continually added to the sacculus throughout life (9). Developing hair cells, each with a diminutive apical surface from which extends a small hair bundle containing a long, isodiametric kinocilium, occur at the macular margin, where the sensory epithelium abuts the surrounding extramacular, or nonsensory, epithelium (9, 10).

Cells in the sensory and nonsensory epithelia are immunolabeled in saccular cryosections by a recombinant antibody fragment, scFv-278, isolated from a bacteriophage-displayed library directed against inner-ear proteins (4). To identify the saccular cells that are recognized by scFv-278, we immunolabeled whole-mounted sacculi and examined them by confocal microscopy. This analysis confirmed the intense labeling of extramacular cells (Fig. 1A), including the cuboidal epithelial cells that line the epithelial sac containing the endolymph and otoconia.

The saccular sensory epithelium displayed a honeycomb pattern of immunoreactivity in which unlabeled cells were encircled by strongly labeled ones (Fig. 1 A and D). To identify the cells containing the antigen, we used fluorescently conjugated phalloidin to mark actin filaments, which are concentrated in mechanosensitive hair bundles (Fig. 1 B and E). Double labeling indicated that the unlabeled cells possessed hair bundles protruding from their apical surfaces (Fig. 1 C and F). The honeycomb appearance therefore resulted from antigen-containing supporting cells punctuated by unlabeled hair cells. At the periphery of the sensory epithelium, small, unlabeled cells were visualized in the zone of hair-cell maturation (9, 10); each unlabeled cell possessed a diminutive hair bundle and hence was an immature hair cell (Fig. 1 A–C).

A few unlabeled cells occurred in the extramacular epithelium; some were hundreds of micrometers from the macula (Fig. 1 G and J). These were confirmed to be small hair cells based on their diminutive hair bundles and actin-rich cuticular plates (Fig. 1 H and I and 1 K and L). We also observed extramacular cells with reduced immunoreactivity, but without detectable hair bundles (data not shown). These may have represented cells that had adopted a hair-cell fate, but whose bundles had not yet begun to develop.

Examination of the seven other hair cell-containing receptor organs of the bullfrog revealed labeling patterns similar to that observed in the sacculus (data not shown). In the utriculus and lagena, however, supporting cells demonstrated little or no immunoreactivity near the striola, the arc at which the morphological polarity of hair cells reverses.

Immunoreactivity of Isolated Hair Cells. Although immunopositive hair cells were not apparent in whole-mounted sacculi, examination of isolated hair cells revealed that some contained small amounts of the antigen. The extent of this immunoreactivity correlated with the maturity of a hair cell, as assessed by the morphological attributes of its hair bundle (10, 11). An immature hair cell, characterized by an elongated soma, short stereocilia, and an extended kinocilium, exhibited perinuclear labeling that often extended toward the apical cellular surface (Fig. 2A). Labeling was eliminated by omission of scFv-278 (Fig. 2B) and was not seen with irrelevant scFvs. A mature hair cell, with a stout soma, large hair bundle, and retracted kinocilium, exhibited no immunoreactivity (Fig. 2D). In a hair cell of intermediate bundle morphology (Fig. 2C), labeling occurred only in the perinuclear region and was reduced in comparison to that of a less mature hair cell.

Identification of the Antigen by Expression Screening. To identify the antigen recognized by scFv-278, we used the scFv to screen a
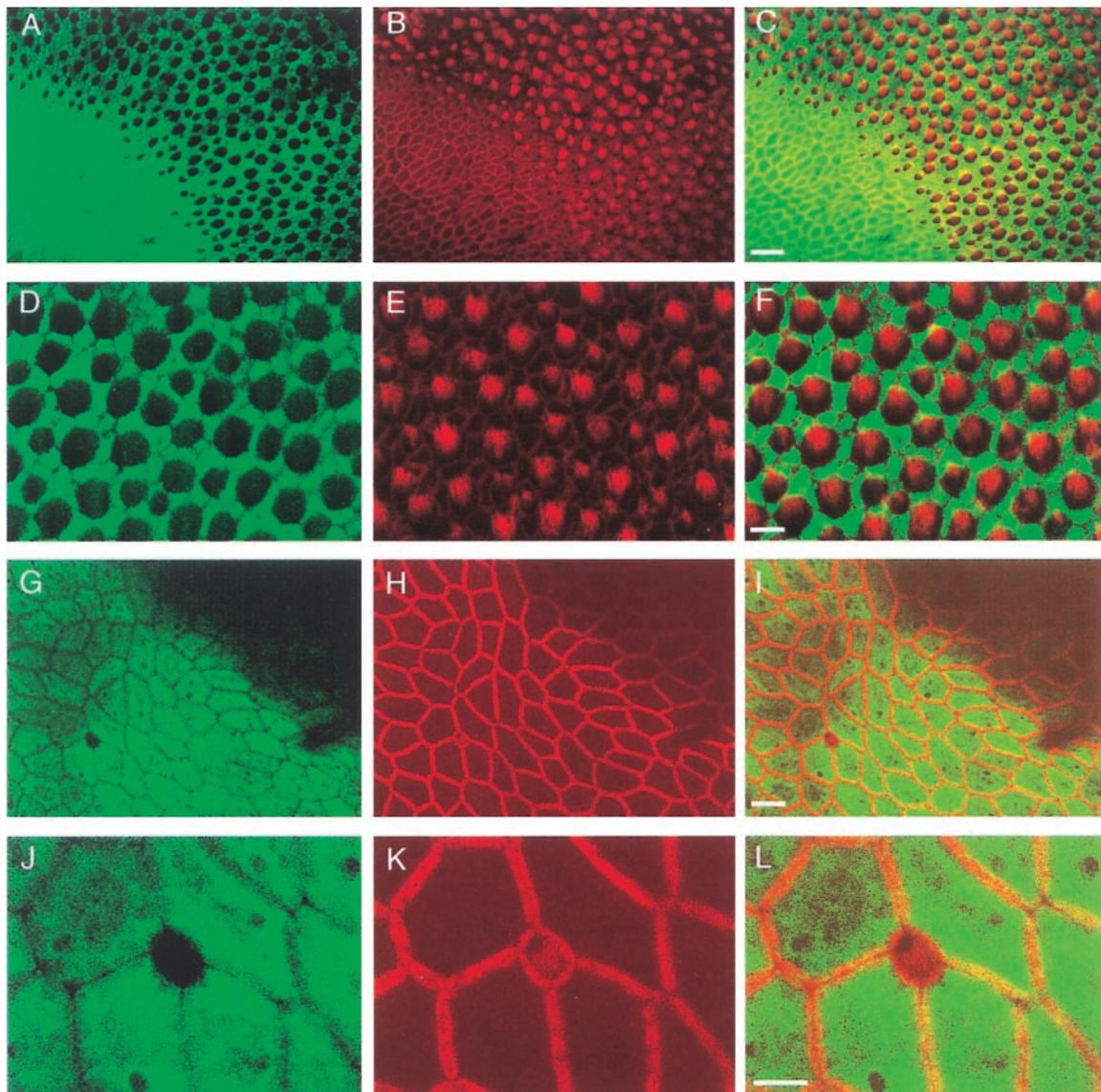
Fig. 1. Double-labeling of the bullfrog sacculus with scFv-278 and tetramethylrhodamine B isothiocyanate-phalloidin. (*A*) Immunolabeling with the scFv reveals intense reactivity in the extramacular epithelium and a honeycomb pattern of labeling within the sensory epithelium. (*B*) Phalloidin labels circumferential actin bands in supporting cells and cells of the extramacular epithelium, as well as the hair bundles of hair cells. (*C*) In a merged image, scFv immunoreactivity is confined to supporting cells and extramacular epithelial cells. (The bar represents 20 μm in *A*–*C*.) (*D*) In the central portion of the sensory epithelium, the scFv strongly labels the supporting cells that surround hair cells. (*E*) Phalloidin demarks hair bundles as well as the circumferential actin rings of supporting cells. (*F*) In a merged image, each cell unlabeled by the scFv possesses a hair bundle and is therefore a hair cell; the labeled cells lack hair bundles and are accordingly supporting cells. (The bar represents 10 μm in *D*–*F*.) (*G*) Small unlabeled cells occur hundreds of micrometers from the sensory epithelium. One such cell is depicted amid a sea of extramacular cells. (*H*) Phalloidin delineates the cortical actin network of the extramacular epithelial cells and the diminutive hair bundle and cuticular plate of the cell lacking immunoreactivity. (*I*) In a merged image, scFv-278 immunoreactivity is evident in the extramacular cells and not the small hair cell. (The bar represents 10 μm in *G*–*I*.) (*J*–*L*) Higher magnification images of the region examined in *G*–*I* depict a solitary hair cell located in the extramacular epithelium. (The bar represents 5 μm in *J*–*L*.)

bullfrog saccular cDNA expression library. Tissue-culture cells were transiently transfected with the mass-excised cDNA library, which had been divided into subpools, and screened for immunoreactive cells. Positive pools were subdivided and retested until a single clone that conferred immunoreactivity was isolated (Fig. 3*A*). Cells transfected with this clone displayed no immunoreactivity when the scFv was omitted (Fig. 3*B*).

Analysis of the isolated cDNA clone revealed an insert of about 2,300 bp. Because this clone did not represent the 5′ end of the mRNA, we used the PCR to amplify the missing portion from the saccular library. The sequence contained the presump-

tive translation-initiation site, which resulted in a predicted ORF encoding a 529-aa protein with a molecular mass of 56 kDa.

Sequence analysis of the predicted protein assigned it to the type II cytokeratin family of intermediate-filament proteins (Fig. 4). The protein displayed the highest degree of aa sequence conservation, 75% identity, with XenCK55(5/6), a cytokeratin from the *Xenopus laevis* esophagus (Fig. 4; ref. 12). The next most similar proteins are otokeratin, a cytokeratin from chicken cochlea (13), which displays 70% aa identity to the inner-ear cytokeratin (Fig. 4), and human cytokeratin 5 (14), which is 62% identical (data not shown). The four cytokeratins are most
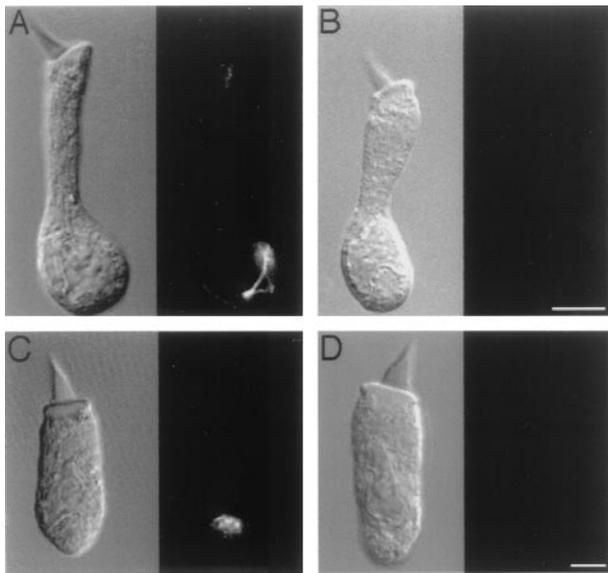
Fig. 2. Confocal images of immunolabeling with scFv-278 in isolated saccular hair cells. (*A*) In a hair cell shown by differential interference contrast microscopy (*Left*) to possess an immature hair bundle, immunoreactivity (*Right*) is concentrated in the perinuclear region of the cytoplasm and extends toward the apical cellular surface. (*B*) In a hair cell possessing an immature hair bundle, no immunolabeling occurs when scFv-278 is omitted. (The bar represents 5 μm in *A* and *B*.) (*C*) In a hair cell with a hair bundle of intermediate development, immunoreactivity occurs only in the perinuclear region. (*D*) A hair cell with a mature hair bundle displays no immunolabeling. (The bar represents 5 μm in *C* and *D*.)

Fig. 3. Mammalian expression cloning and epitope mapping of the antigen recognized by scFv-278. (*A*) Immunocytochemical labeling demonstrates scFv-278 immunoreactivity of cells transfected with the cDNA clone isolated from a bullfrog saccular expression library. Transfected cells, demarked by a colored reaction product, and untransfected cells are shown. (*B*) Cells transfected with the isolated cDNA clone are not labeled when the scFv is omitted. (*C*) Transfection with a construct (Δ481–529) whose product was truncated after aa 480 yields immunopositive cells, indicating that the epitope does not lie in the carboxyl-terminal region. (*D*) Transfection with a construct (EGFP:168–393:FLAG) that contains cytokeratin residues 168–393 results in immunopositive cells. The epitope therefore occurs in the relatively conserved α-helical coiled-coil domain of the molecule.

similar in the predicted α-helical coiled-coil regions that mediate filament assembly; their sequences diverge at the carboxyl termini and to a lesser extent at the amino termini.

The high degree of similiarity between bullfrog cytokeratin and the XenCK55(5/6) protein, in conjunction with the presence of scFv-278 immunoreactivity in cryosections of bullfrog esophagus, led us to examine the presence of the antigen in *Xenopus* tissues. Although significantly reduced by comparison to that seen in the bullfrog sacculus, immunoreactivity was observed in cryosections of *Xenopus* esophagus (data not shown). Examination of whole-mounted *Xenopus* sacculi, however, revealed no immunolabeling; the expression of cytokeratin in the inner ear may therefore be species-specific. Confirming the immunocytochemical results, immunoblots of homogenates of the inner ear, esophagus, eye, heart, liver, and skin from *Xenopus* and bullfrogs showed a single band corresponding to a molecular mass of slightly less than 50 kDa only in the bullfrog inner ear and to a lesser extent the esophagus (Fig. 5).

Localization of the Epitope Recognized by scFv-278. The specificity of scFv-278 for a cytokeratin in the inner ear prompted a search for the epitope it recognized. Deletion constructs of the cytokeratin were used to transfect tsA201 cells, which were then processed for immunocytochemistry. A construct encoding a protein truncated after aa 480 (Δ481–529) conferred immunoreactivity on transfected cells (Fig. 3*C*); the residues involved in scFv binding thus do not occur near the protein carboxyl terminus. Although the corresponding protein was synthesized, transfection with a construct expressing aa 66–169 yielded no immunoreactivity (data not shown). Immunoreactivity did occur, however, after transfection with a construct (EGFP:168–393:FLAG) in which aa 168–393 and an epitope tag were fused to the carboxyl terminus of EGFP (Fig. 3*D*). These data suggest that scFv binding occurs between aa 168 and 393, the predicted α-helical

coiled-coil domain. Although this region is highly conserved, small pockets of divergence exist. Several of these areas are predicted to be unstructured and may thus be antigenic; an epitope in one of these divergent regions would explain the specificity of our reagent.

Ultrastructural Localization of Cytokeratin Immunoreactivity. Immunoelectron microscopy provided independent evidence to support the identification of the antigen as a cytokeratin. Although many of the subcellular structures were extracted by the rigorous preparative procedure, the gold particles marking immunoreactivity were consistently observed in the intermediate-filament networks at the apices of extramacular cells (Fig. 6*A*). In accordance with the light-microscopic observations, the apices of supporting cells were also labeled (Fig. 6*B*), albeit to a lesser extent than those of extramacular cells. In both cell types, labeling was absent from nuclei, microvilli, and the circumferential actin rings associated with junctional complexes. No labeling was observed in hair cells (data not shown).

Discussion

A Cytokeratin Expressed in the Inner Ear. From a library of antibody fragments displayed on the surface of bacteriophage, we have previously isolated a reagent that specifically recognizes an inner-ear protein (4). This protein, which is found predominately in inner-ear tissues, has been identified by expression cloning as a member of the cytokeratin class of intermediate-filament proteins. This identification is supported by the immunolocalization of the antigen to 10-nm filaments by immunoelectron microscopy and the concordance of the predicted size of the cloned antigen with the apparent molecular mass of a protein immunolabeled on blots of inner-ear proteins.

Cyr et al.

Fig. 4. Amino acid sequence of the cytokeratin recognized by scFv-278. The predicted aa sequence of the antigen, here denoted ''BFcytokeratin'', is aligned with those of the two most closely related proteins described heretofore, the cytokeratins XenCK55(5/6) and otokeratin. The residues of the inner-ear cytokeratin and identical residues in the other proteins appear in reverse contrast; dashes represent gaps and periods denote stop codons. The predicted α-helical coiled-coil domain of BFcytokeratin extends from residues 131 to 446. The original cytokeratin clone extended only to the codon for residue 66; the remaining 5′ sequence was isolated by using a PCR-based strategy.

The functions of cytokeratins are incompletely understood. Although they provide mechanical stability to cells, cytokeratins probably serve other roles as well, including the organization of organelles and the nucleus (15–17). Cytokeratins, including cytokeratins 8, 9, and 19 and otokeratin, are known to occur in cells of the inner ear (13, 18–23). A definitive subclassification of our inner-ear cytokeratin within the type II cytokeratin family is difficult because of the sequence conservation within this family and the lack of anuran cytokeratin sequences to use for comparison. Although the inner-ear cytokeratin exhibits homology to cytokeratin 5, which is abundantly expressed in the skin (24), the absence of immunoreactivity in cryosections (data not shown) and immunoblots of bullfrog skin suggests that the inner-ear clone is not the bullfrog ortholog of human cytokeratin 5. The distinction between bullfrog inner-ear cytokeratin and XenCK55(5/6) or otokeratin is less obvious. Although the bullfrog inner-ear cytokeratin may be an ortholog of one or both of these molecules, the sequence divergence at the amino and carboxyl termini, regions that are diagnostic of cytokeratin class distinctions, argues against this possibility and suggests that this is a new member of this subfamily of proteins that is highly related to cytokeratins 5 and 6.

A Marker for Differentiation of Hair Cells. During development and regeneration, new hair cells arise from the division of supporting cells, some of whose progeny retain a supporting-cell identity whereas others assume a hair-cell fate (25–31). After damage to some receptor organs, hair-cell replacement in the absence of cell division suggests that supporting cells can also transdifferentiate directly into hair cells (29, 32, 33).

A thorough dissection of the steps of differentiation has been hampered by the shortage of markers with which to track the progression of nonsensory into sensory cells. Immunological reagents that preferentially label specific cell types of the inner ear may prove helpful in this context. The anti-cytokeratin scFv should be useful in delineating the stages of hair-cell differentiation in the bullfrog sacculus. The correlation of immunoreactivity with hair-bundle morphology, a signature of hair-cell maturation, strongly suggests that expression of the cytokeratin is down-regulated or the protein is degraded or modified during hair-cell differentiation. If the extramacular cells with reduced immunoreactivity are destined to become sensory cells, the decline in labeling precedes bundle development and therefore provides a very early index of hair-cell fate.

Although the role of the cytokeratin in the inner ear is unclear, the reduced expression of this protein during hair-cell differentiation is intriguing. When basal cells in the epidermis begin to differentiate by withdrawing from the cell cycle and migrating away from the basal lamina, cytokeratin expression is altered, including a down-regulation of cytokeratin 5 (24). As hair cells differentiate and lose contact with the basal lamina, their specific cytokeratin, which is similar to cytokeratin 5, displays an analogous down-regulation. Unlike the cells of the epidermis, how-
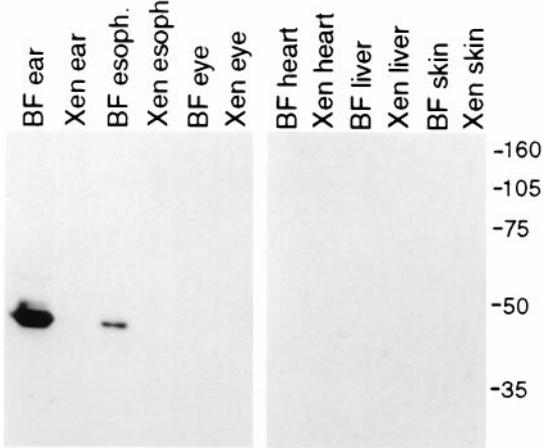
Fig. 5. Labeling of the cytokeratin on immunoblots of homogenates from bullfrog and *Xenopus* organs. Immunoblots of protein homogenates from bullfrog (denoted ''BF'') and *Xenopus* (denoted ''Xen'') organs reveal a single band recognized by the anti-cytokeratin scFv only in the bullfrog inner ear and esophagus. Molecular mass markers in kilodaltons are indicated at the right and apply to both blots.
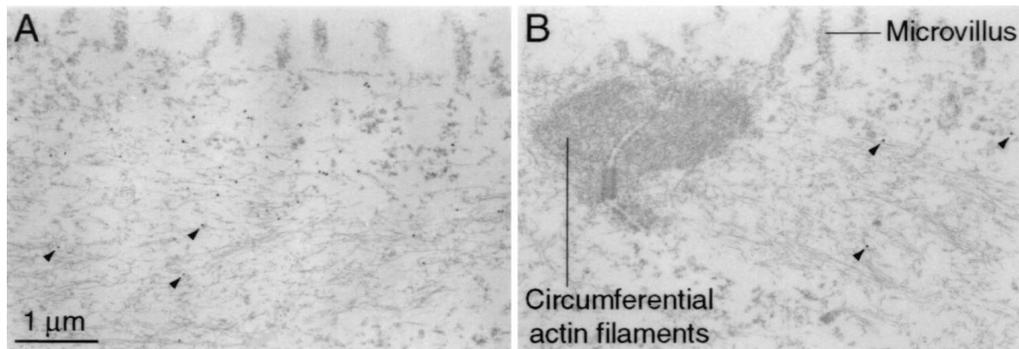
Fig. 6. Immunoelectron microscopic localization of the inner-ear cytokeratin to intermediate filaments in saccular cells. (*A*) Immunogold labeling of extramacular cells of the sacculus with the anti-cytokeratin scFv reveals numerous gold particles, three of which are indicated with arrowheads, on 10-nm filaments in the apical portion of the cell. Because of the extensive cellular permeabilization, many subcellular structures have been extracted; intermediate filaments and actin filaments persist. Note the lack of labeling of the microvilli located at the cellular apex. The scale bar pertains to both panels. (*B*) Within supporting cells, immunolabeling can be detected on cytoplasmic filaments located at the cellular apex; arrowheads demark the three gold particles in this section. Microvilli and the circumferential actin filaments associated with the junctional complex are unlabeled. In corroboration of the light microscopic observations, the immunoreactivity of supporting cells is weaker than that of extramacular cells.

ever, hair cells do not appear to express other forms of cytokeratin when they terminally differentiate.

As a hair cell matures, a reorganization of the cytoskeleton must occur to produce an exquisitely sensitive sensory cell. The growth of a hair bundle with its actin-filled stereocilia is the most obvious cytoskeletal alteration, but subtler changes must occur as well, including the removal of the apical network of intermediate filaments. Although it is improbable that the loss or modification of the cytokeratin described here triggers the acquisition of a sensory phenotype, this protein evidently plays a role in nonsensory cells that is unnecessary in hair cells and its altered expression provides a useful index of hair-cell differentation.

1. Hudspeth, A. J. (1997) *Neuron* **19,** 947–950.
2. Corwin, J. T. & Oberholtzer, J. C. (1997) *Neuron* **19,** 951–954.
3. Stone, J. S., Oesterle, E. C. & Rubel, E. W. (1998) *Curr. Opin. Neurol.* **11,** 17–24.
4. Cyr, J. L. & Hudspeth, A. J. (2000) *Proc. Natl. Acad. Sci. USA* **97,** 2276–2281.
5. Perez, C. & Kriegler, M. (1990) *Resolutions* **6,** 1–2.
6. Margolskee, R. F., McHendry-Rinde, B. & Horn, R. (1993) *BioTechniques* **15,** 906–911.
7. Koyama, H., Lewis, E. R., Leverenz, E. L. & Baird, R. A. (1982) *Brain Res.* **250,** 168–172.
8. Yu, X., Lewis, E. R. & Feld, D. (1991) *J. Comp. Physiol. A* **169,** 241–248.
9. Corwin, J. T. (1985) *Proc. Natl. Acad. Sci. USA* **82,** 3911–3915.
10. Li, C. W. & Lewis, E. R. (1979) *Ann. Otol.* **88,** 427–437.
11. Kelley, M. W., Ochiai, C. K. & Corwin, J. T. (1992) *Hear. Res.* **59,** 108–115.
12. Fouquet, B., Herrmann, H., Franz, J. K. & Franke, W. W. (1988) *Development (Cambridge, U.K.)* **104,** 533–548.
13. Heller, S., Sheane, C. A., Javed, Z. & Hudspeth, A. J. (1998) *Proc. Natl. Acad. Sci. USA* **95,** 11400–11405.
14. Eckert, R. L. & Rorke, E. A. (1988) *DNA* **7,** 337–345.
15. McConnell, S. J. & Yaffe, M. P. (1993) *Science* **260,** 687–689.
16. Chan, Y.-M., Anton-Lamprecht, I., Yu, Q.-C., Jäckel, A., Zabel, B., Ernst, J.-P. & Fuchs, E. (1994) *Genes Dev.* **8,** 2574–2587.
17. Sarria, A. J., Lieber, J. G., Nordeen, S. K. & Evans, R. M. (1994) *J. Cell Sci.* **107,** 1593–1607.
18. Raphael, Y., Marshak, G., Barash, A. & Geiger, B. (1987) *Differentiation (Berlin)* **35,** 151–162.
19. Anniko, M. & Arnold, W. (1990) *Acta Otolaryngol. Suppl.* **470,** 40–50.
20. Bauwens, L. J. J. M., Veldman, J. E., Bouman, H., Ramaekers, F. C. S. & Huizing, E. H. (1991) *Ann. Otol. Rhinol. Laryngol.* **100,** 211–218.
21. Raphael,Y. & Altschuler, R. A. (1991) *Cell Motil. Cytoskeleton* **18,** 215–227.
22. Usami, S.-I., Hozawa, J., Shinkawa, H., Saito, S.-I., Matsubara, A. & Fujita, S. (1993) *Acta Otolaryngol. Suppl.* **506,** 7–13.
23. Mogensen, M. M., Henderson, C. G., Mackie, J. B., Lane, E. B., Garrod, D. R. & Tucker, J. B. (1998) *Cell Motil. Cytoskeleton* **41,** 138–153.
24. Fuchs, E. (1996) *Annu. Rev. Genet.* **30,** 197–231.
25. Corwin, J. T. & Cotanche, D. A. (1988) *Science* **240,** 1772–1774.
26. Ryals, B. M. & Rubel, E. W. (1988) *Science* **240,** 1774–1776.
27. Balak, K. J., Corwin, J. T. & Jones, J. E. (1990) *J. Neurosci.* **10,** 2502–2512.
28. Weisleder, P., Tsue, T. T. & Rubel, E. W. (1995) *Hear. Res.* **82,** 125–133.
29. Jones, J. E. & Corwin, J. T. (1996) *J. Neurosci.* **16,** 649–662.
30. Warchol, M. E. & Corwin, J. T. (1996) *J. Neurosci.* **16,** 5466–5477.
31. Fekete, D. M., Muthukumar, S. & Karagogeos, D. (1998) *J. Neurosci.* **18,** 7811–7821.
32. Baird, R. A., Steyger, P. S. & Schuff, N. R. (1996) *Ann. N.Y. Acad. Sci.* **781,** 59–70.
33. Adler, H. J., Komeda, M. & Raphael, Y. (1997) *Int. J. Dev. Neurosci.* **15,** 375–385.

NEUROBIOLOGY